JOURNAL OF CATALYSIS 96, 429–438 (1985)

Preparation Chemistry of Precipitated Ni–SiO_2 Catalysts for Enantioselective Hydrogenation

YURIKO NITTA, TOSHINOBU IMANAKA, AND SHIICHIRO TERANISHI

Department of Chemical Engineering, Faculty of Engineering Science, Osaka University, Toyonaka, Osaka, 560 Japan

Received April 5, 1985; revised June 28, 1985

Effects of preparation conditions on chemical composition and reducibility of precipitated precursors of Ni–SiO_2 catalysts were studied using thermal gravimetric analysis. The proportion of $NiCO_3$ in the precursor decreased as the preparation conditions became severe and the reducibility of the precursor decreased with a decrease in the $NiCO_3$ content, suggesting stronger metal–support interaction of SiO_2 with $Ni(OH)_2$ than with $NiCO_3$. The X-ray diffraction measurements showed that the mean crystallite size of nickel in H_2-reduced catalysts increased with increasing $NiCO_3$ content in the precursor. The activity and selectivity of the modified catalysts in enantioselective hydrogenation of methyl acetoacetate depended on the proportion of $NiCO_3$ in the precursor and were explained in terms of crystallite size distribution of nickel in the catalysts.

INTRODUCTION

Preparation methods and conditions of supported nickel catalysts and their effects on the catalytic properties have been studied by so many groups for more than 25 years because of their important role in hydrogenation and hydrogenolysis reactions (*1–13*). Impregnation, coprecipitation, ion-exchange, and homogeneous precipitation methods have been most widely used, while simple precipitation method seems to have received less attention so far.

Precipitation of metal salts with sodium carbonate in the presence of suspended supports is one of the typical and convenient methods for the preparation of supported metal catalysts. Activity and selectivity of these precipitated catalysts are known to vary considerably by changes in the preparation conditions, probably because of the change in composition of the precipitate (basic metal carbonate) (*14*). However, the relation between the composition of these catalyst precursors and preparation conditions have not been evaluated quantitatively, and the effects of the composition of precursors on the activity and selectivity of the H_2-reduced catalysts have not been discussed in detail.

In the enantioselective hydrogenation of methyl acetoacetate (MAA) to methyl 3-hydroxybutyrate (MHB) on tartaric acid-modified nickel catalysts, we reported that the enantioselectivity of the catalysts increases with an increase in the mean crystallite size of nickel (*15*). With supported nickel catalysts, we showed that almost all preparation variables such as precipitation temperature affect the selectivity of the modified catalysts, and suggested a change in the crystallite size distribution (CSD) of nickel with a change in preparation conditions (*16, 17*). Therefore, the effects of preparation variables on the composition of catalyst precursors and also the dependence of the CSD of nickel on the composition of precursors should be clarified next.

In the present study, we examined the effects of preparation variables on the chemical composition and on the reducibility of the catalyst precursors by means of thermal gravimetric analysis (TGA). The X-ray diffraction (XRD) patterns of hydrogen-

0021-9517/85 $3.00

reduced or calcined catalysts were measured in order to reveal the influence of the composition of catalyst precursors on the morphology of the resulting catalysts. The enantioselectivity as well as the activity of the modified Ni–SiO_2 catalyst was found to depend on the proportion of $NiCO_3$ in the catalyst precursor and was explained in terms of the CSD of nickel in the catalyst (*18*).

EXPERIMENTAL

Catalyst Preparation

Most catalyst precursors were prepared by a precipitation method with Na_2CO_3 from aqueous $Ni(NO_3)_2$ solution suspended by silica gel (Nakarai Chemicals, No. 1, 60–200 mesh, 600 m^2/g). The molar ratio of Na_2CO_3 to nickel salt, the precipitation temperature, aging time, drying temperature, and drying time were changed to prepare precursors with different compositions. The nickel weight loading (usually 50%) was sometimes changed by varying the concentration of the $Ni(NO_3)_2$ solution. Sodium hydroxide was used as a precipitant to prepare a precursor free from carbonate for comparison. In preparing a standard sample precipitation was carried out at 75°C by use of equimolar alkali with nickel salt, followed by aging for 15 min, washing three times with warm distilled water, and drying in air at 110°C for 20–24 h. Other details for the preparation of precursors were described elsewhere (*16*). Two grams of a Ni–SiO_2 (1 : 1) precursor (containing ca. 0.7 g of Ni) was reduced in a H_2 stream of 8 liters/h at 400°C for 3 h unless otherwise stated. After cooling to ambient temperature with the H_2 gas still flowing, the catalyst was modified with aqueous tartaric acid solution according to the method described previously (*16, 19*) and was rinsed with distilled water and methanol before use in hydrogenation reactions.

Analysis

The TG measurements of catalyst precursors were carried out using a Shimadzu DT-30 thermal analyzer. Freshly prepared samples (40 mg each) were heated either in N_2 or H_2 flow to 600°C at a temperature ramp of 5°C/min. Measurements in H_2 flow were also performed up to 400°C at a temperature ramp of 10°C/min followed by keeping this temperature for 3 h, in order to get information on the percentage reductions of the catalysts used in hydrogenation reactions. In TGA experiments, both weight loss (TG) and the first derivative of weight loss (DTG) were monitored. The XRD patterns of the catalysts were measured with a Shimadzu VD-1 diffractometer after separation from the reaction mixture. The mean crystallite size ($\overline{D}_c$) of nickel was calculated from the half-width of the peak on (111) plane of nickel metal. The XRD patterns were also measured for the precursors calcined in N_2 at 400°C for 2 h . The CSDs of nickel in the catalysts were computed by the numerical analysis method described by Moraweck *et al.* (*20*) for X-ray line profile analysis, setting the number of polynomial coefficients to 5 and tentatively neglecting the lattice strain contribution to the broadening of the X-ray line. The BET surface areas and metal surface areas of some catalysts were measured by N_2 adsorption at −196°C and by H_2 adsorption at 20°C, respectively.

Hydrogenation

Ten milliliters of MAA in 10 ml of ethyl acetate was hydrogenated with the modified catalyst at 60°C under a starting H_2 pressure of 10 kg/cm^2 by using a glass autoclave (TEM-U-50, Taiatsu Glass Industry Co.) equipped with a magnetic stirring system. The H_2 pressure decreased to about 3 kg/cm^2 at 100% conversion. The hydrogenation activity of the catalyst was determined from the pressure decrease during the initial 15 min of the reaction. The optical yield (OY) of MHB determined from the optical rotation of distilled product was employed as a measure of the selectivity of the catalyst.

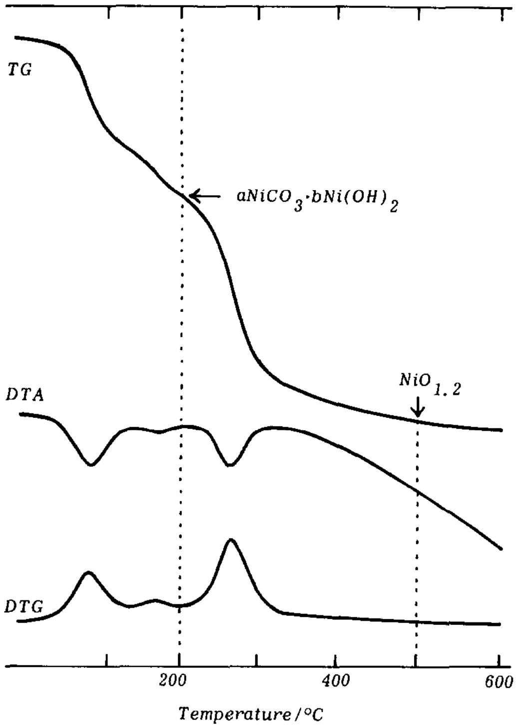

FIG. 1. Thermal decomposition of the standard precursor of Ni–SiO$_2$ (1 : 1) catalyst in N_2 flow. TG, weight loss in thermal gravimetric measurements; DTG, first derivative of the weight loss; DTA, differential thermal analysis.

RESULTS AND DISCUSSION

Thermogravimetric Analysis of Catalyst Precursors

Figure 1 shows a typical TGA profile of the standard precursor measured in N_2 flow. The differential thermal gravimetric (DTG) curve, i.e., first derivative of the weight loss (TG) curve, has peaks exactly corresponding to the endothermic changes in differential thermal analysis (DTA). Therefore, we confine our attention to the DTG profiles hereafter. The peak around 70–100°C corresponds to the weight loss due to the desorption of water adsorbed mainly on silica gel. The small peak around 150°C is attributable to the water of crystallization of nickel carbonate. The decomposition of basic nickel carbonate to nickel oxide is indicated by the peak around 270°C. The decarboxylation of unsupported basic nickel carbonate to nickel oxide occurs at a higher temperature than the dehydration of unsupported nickel hydroxide as shown in Fig. 2. The percentage weight loss for the decarboxylation of $NiCO_3$ is larger than that for the dehydration of $Ni(OH)_2$. Accordingly, from the location of the DTG peaks shown in Fig. 2 and the extent of the weight loss corresponding to the decomposition of basic nickel carbonate to nickel oxide, we can conclude that the proportion of $NiCO_3$ in the precursors decreases with an increase in drying temperature. This is probably because the following reaction is accelerated by a rise in temperature, especially in the presence of silica gel.

$$\begin{aligned} &a\mathrm{Ni(OH)_2} \cdot b\mathrm{NiCO_3} \cdot \mathrm{aq} \\ &\quad + x\mathrm{H_2O} \rightarrow (a + x)\mathrm{Ni(OH)_2} \\ &\qquad \cdot (b - x)\mathrm{NiCO_3} \cdot \mathrm{aq} + x\mathrm{CO_2} \end{aligned}$$

Similarly, increases in the amount of added alkali (i.e., pH of the solution), precipitation temperature, aging time, and drying time were found to decrease the proportion

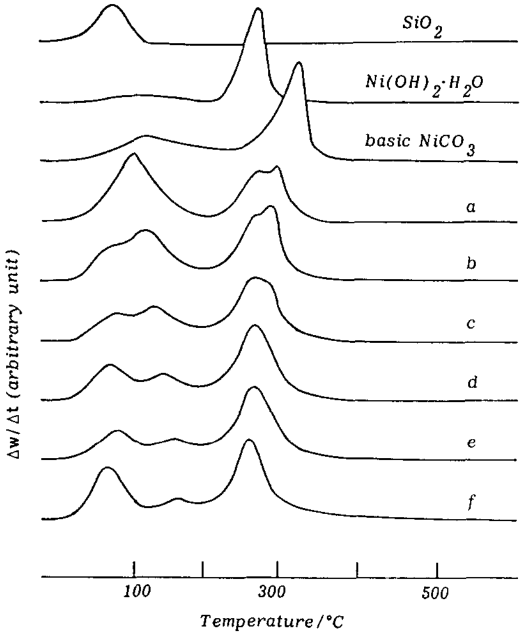

FIG. 2. DTG-in-N_2 profiles of the catalyst precursors dried at (a) 50°C, (b) 70°C, (c) 90°C, (d) 100°C, (e) 110°C, and (f) 120°C.

TABLE 1

Effect of Preparation Conditions on the Composition of Catalyst Precursors

Run No.	Preparation conditions					$NiCO_3$ content[b] in precursor (%)
	Ppt. temp. (°C)	$\frac{\text{Ni}^a}{\text{Alkali}}$	Aging time (min)	Drying temp. (°C)	Drying time (h)	
1	75	1.0	15	70	20	49
2	75	1.0	15	90	20	45
3	75	1.0	15	100	20	41
4[c]	75	1.0	15	110	20	37
5	75	1.0	15	120	20	34
6	0	1.0	15	110	24	38
7	85	1.0	15	110	24	27
8	75	1.2	15	110	24	41
9	75	0.8	15	110	24	32
10	75	1.0	0	110	24	37
11	75	1.0	60	110	24	30
12	0	1.2	0	20[d]	72	78
13	0	1.2	0	50	20	61
14	85	0.8	30	110	45	18
15	90	0.8	60	120	48	7

[a] Molar ratio of nickel nitrate to sodium carbonate.
[b] Molar percentage of $NiCO_3$ in $a\mathrm{Ni(OH)_2} \cdot b\mathrm{NiCO_3}$.
[c] Standard conditions except drying time.
[d] Evacuated for 3 h and dried on $CaCl_2$.

of $NiCO_3$ in the precursors. The molar percentages of $NiCO_3$ in the basic nickel carbonates were quantitatively estimated from the weight losses in the range of 200 to 500°C which correspond to the following reactions (*21*): $NiCO_3 \rightarrow NiO_{1.2}$ and $Ni(OH)_2 \rightarrow NiO_{1.2}$. The results are listed in Table 1. The $NiCO_3$ percentage in a precursor prepared under the standard conditions was around 35%. The milder preparation conditions resulted in the higher proportion of $NiCO_3$ in the precursor. Now the selection of preparation conditions made it possible to prepare precursors with desired $NiCO_3$ percentage in the range from ca. 5–80% as illustrated in Table 1 (Runs 12–15).

Interaction between Nickel Salt and SiO_2

Figure 3 shows the DTG profiles of the precursors with different nickel loadings prepared under the standard conditions. It is apparent that the proportion of $NiCO_3$ in the precursor increases with increasing nickel loading. Wendt *et al.* showed that DTA peaks of nickel hydroxide on SiO_2 are shifted to higher temperature with increasing SiO_2 content probably by incorporation of nickel layer silicate (*22*). Therefore, it is supposed that the interaction of the support with nickel precipitate accelerates the change of $NiCO_3$ to $Ni(OH)_2$ in the initial stage of precipitation, whereas additional precipitate, having no interaction with support, remains as $NiCO_3$. As for the precursors with a constant nickel loading (i.e., 50%), the decomposition temperature of the nickel precipitate became higher with increasing proportion of $Ni(OH)_2$, especially beyond ca. 65%, as shown in Fig. 4. This means that the interaction between $Ni(OH)_2$ and SiO_2 becomes stronger with increasing proportion of $Ni(OH)_2$ as the preparation conditions become severe. In the case of unsupported basic nickel carbonate, the $NiCO_3$ content did not vary so much with a change in preparation conditions. Moreover, the decomposition of

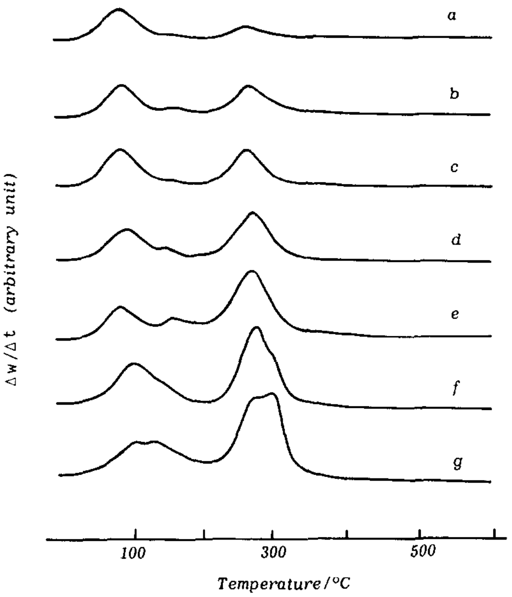

FIG. 3. DTG-in-N_2 profiles of the catalyst precursors with various nickel loadings: (a) 17%, (b) 23%, (c) 33%, (d) 43%, (e) 50%, (f) 67%, and (g) 80%.

SiO_2-supported $Ni(OH)_2$ prepared by using NaOH as a precipitant took place slowly at a higher temperature than that of unsupported $Ni(OH)_2$. These findings also support the presence of strong interaction between SiO_2 and $Ni(OH)_2$ in the precursor. Many groups have shown that the method of preparation affects the physical and chemical characteristics of the resulting catalysts including the degree of precursor–support interaction. Our work indicates that not only preparation methods but also preparation conditions such as precipitation and drying temperatures can affect the properties of the resulting catalysts. Hermans and Geus (*8*) also reported that the difference in the precipitation temperature of homogeneous precipitation method leads to the different nickel species on SiO_2 support.

Reducibility of the Precursors

The DTG profiles measured under H_2 flow are shown in Fig. 5 for various precur-

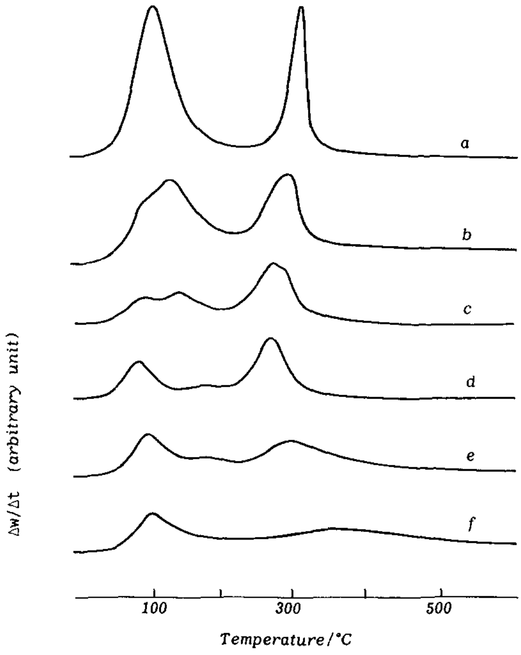

FIG. 4. DTG-in-N_2 profiles of the various precursors with different $NiCO_3$ contents: (a) 78%, (b) 56%, (c) 45%, (d) 35%, (e) 18%, and (f) 7%.

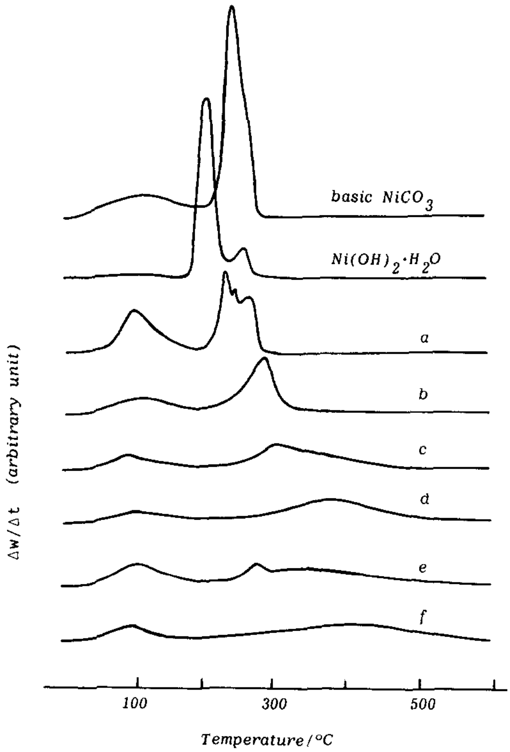

FIG. 5. DTG-in-H_2 profiles of the various precursors with different $NiCO_3$ contents: (a) 78%, (b) 45%, (c) 18%, (d) 7%, (e) 0% (precipitated by NaOH under mild conditions), and (f) 0% (precipitated by NaOH under severe conditions).

sors with different $NiCO_3$ contents, together with the profiles of commercial nickel hydroxide and basic nickel carbonate. The peak around 100–200°C corresponds to the weight loss due to the desorption of adsorbed and crystallization waters, as in the profiles measured under N_2 flow. The reduction of nickel carbonate in the precursor starts at around 200°C and reaches a maximum at 230°C when the $NiCO_3$ content is high, which resembles closely the reduction of unsupported basic nickel carbonate. The smaller peaks around 245 and 265°C may be attributed to the reduction of $Ni(OH)_2$ and $NiCO_3$ having weak support interactions as suggested previously (*8*), although it is difficult for us to assign them exactly. When the heating rate was increased from 5 to 10°C/min, the reduction of nickel carbonate started at a ca. 40°C higher temperature and the two smaller peaks were superposed on the main peak. With decreasing percentage of $NiCO_3$ in the precursor, the reduction peak is shifted to a higher temperature and becomes smaller and broader, indicating that the reduction of nickel precursor to nickel metal becomes difficult with decreasing $NiCO_3$ (i.e., increasing $Ni(OH)_2$) content in the precursor. The reduction of unsupported nickel hydroxide starts at a lower temperature than basic nickel carbonate (*23*) and supported nickel hydroxide as shown in Fig. 5. Moreover, supported nickel hydroxide prepared under mild conditions exhibited two reduction peaks in DTG profile (curve e), one for $Ni(OH)_2$ having weak interaction with support and another for that having strong interaction, whereas the one prepared under severe conditions has only one broad peak for $Ni(OH)_2$ having strong support interaction (curve f). Accordingly, it is clear that the strong interaction between $Ni(OH)_2$ and SiO_2 in a precursor prepared under severe conditions, discussed above, retards the reduction of the precursor probably due to the formation of nickel hydrosilicate. Blackmond and Ko (*13*) suggested that the Ni–SiO_2 catalysts prepared by homogeneous deposition–precipitation at 90°C exhibit layered silicate structures which make it more difficult to reduce the metal precursor species. XPS investigations reported by Lorenz *et al.* (*24*) also showed the formation of nickel layer-silicates in the process of precipitation with dilute ammonia solution. Montes *et al.* (*12, 25*) reported the presence of a strong interaction between metal and support in the case of Ni–SiO_2 precursors prepared by homogeneous precipitation, which gave rise to a nickel hydrosilicate of turbostratic texture. Hermans and Geus (*8*) also reported that nickel hydrosilicate is formed abruptly in the precursors prepared by homogeneous precipitation at 90°C whereas the precipitation at 25°C results in the growth of nickel hydroxide that contains an amount of silicate.

The degree of reduction of a catalyst was evaluated from the weight loss in the range from 200°C to a certain temperature based on the theoretical weight loss for 100% reduction of the precursor examined. The results for the catalysts reduced at a tem-

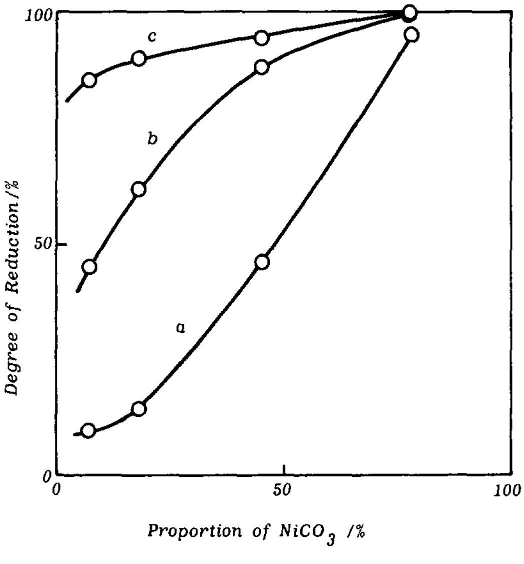

FIG. 6. Dependence of the degrees of reduction on the composition of catalyst precursors. Samples were heated in a H_2 stream of 8 liters/h at a temperature ramp of 10°C/min to (a) 300°C, (b) 400°C, and (c) 400°C and kept there for 3 h.

perature ramp of 10°C/min are shown in Fig. 6 as a function of the NiCO$_3$ percentage in the precursors. The reduction degree of a catalyst heated to 300°C (curve a) increased nearly in proportion to the NiCO$_3$ content in the precursor. This again indicates that NiCO$_3$ in the precursor is free from interaction with support and reduced readily. In the case of a precursor with large NiCO$_3$ content, i.e., prepared under mild conditions, some part of Ni(OH)$_2$ also reduced below 300°C, indicating the presence of Ni(OH)$_2$ which has only weak interaction with support. The proportion of Ni(OH)$_2$ having strong support interaction seems to increase with increasing Ni(OH)$_2$ content in the precursor as the preparation conditions become severe. The reducibility of a precursor with a large Ni(OH)$_2$ content was considerably low when the reduction temperature was below 400°C, although the reduction degrees of the catalysts used in the hydrogenation reactions (i.e., the catalysts reduced at 400°C for 3 h) were all larger than 80%.

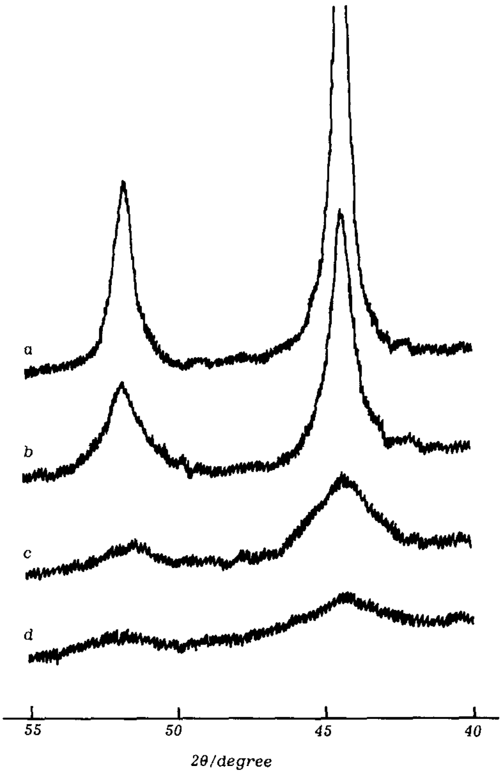

FIG. 7. XRD patterns for H$_2$-reduced catalysts obtained from various precursors with different NiCO$_3$ contents: (a) 61%, (b) 37%, (c) 18%, and (d) 0% (precipitated by NaOH under standard conditions).

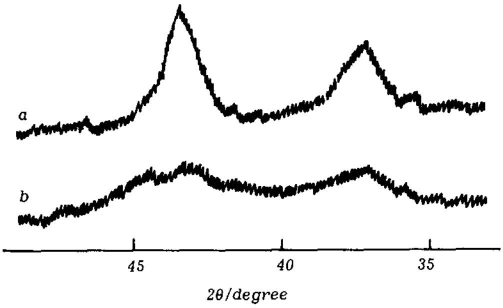

FIG. 8. XRD patterns for the calcined catalysts obtained from (a) NiCO$_3$ 61% and (b) NiCO$_3$ 18% precursors.

Crystallinity of the Reduced Catalysts

The XRD patterns of the H$_2$-reduced catalysts obtained from various precursors with different NiCO$_3$ contents were examined to make clear the influence of the composition of precursors on the crystallinity of nickel metal in the catalysts. As shown in Fig. 7, the crystallinity of a H$_2$-reduced catalyst becomes lower with decreasing proportion of NiCO$_3$ in the precursor. This finding is consistent with the low reducibility of the precursor with a low NiCO$_3$ content as discussed above. The XRD patterns of nickel oxide in two calcined precursors which originally have different proportions of NiCO$_3$, i.e., (a) 61% and (b) 18%, are shown in Fig. 8 for comparison. The crystallinity of the nickel oxide also depended on the composition of precursors; precursor (a) produced nickel oxide with relatively large $\overline{D}_c$ (6 nm) and precursor (b) led to almost amorphous nickel oxide. Subsequent reduction of these calcined precursors resulted in the Ni–SiO$_2$ catalysts which have quite similar XRD patterns to those of the directly reduced catalysts. Richardson and Dubus (5) also reported that calcination of homogeneously precipi-

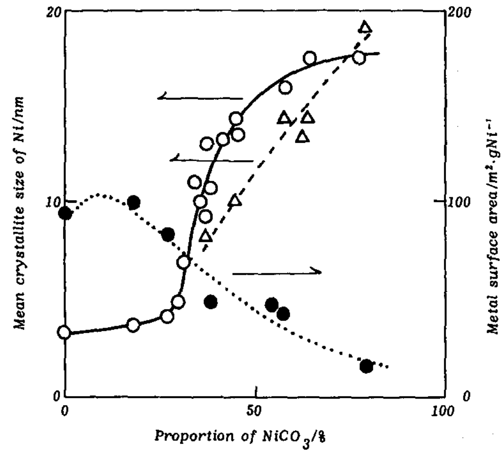

FIG. 9. Dependence of the mean crystallite sizes of nickel (○, △) and the metal surface areas (●) on the composition of catalyst precursors. (○, ●) Reduced at 400°C for 3 h; (△) reduced at 300°C for 1 h.

tated Ni–SiO_2 precursors has no effect on the resulting CSDs of Ni. Therefore, the difference in the crystallinity of nickel among the catalysts obtained from different precursors seems to be due to the difference in the crystallinity of nickel oxide which may be present as an intermediate species in the course of the reduction process. The interaction between $Ni(OH)_2$ and SiO_2 may cause the low crystallinity of nickel oxide and consequently the small $\bar{D}_c$ of nickel after H_2 reduction. This idea is consistent with the previously proposed schemes (*10, 12*) for the reduction process of some Ni–SiO_2 catalyst precursors.

The mean crystallite sizes of nickel metal in the H_2-reduced catalysts, determined by the X-ray line broadening, are shown in Fig. 9 as a function of the $NiCO_3$ content in the precursor. The metal surface area decreased in accord with the increase in $\bar{D}_c$ as the $NiCO_3$ content in the precursor increased, while the BET surface areas did not depend so much on the composition of the precursors as shown in Table 2. Crystallite size distributions of nickel metal, determined by X-ray line profile analysis, are shown in Fig. 10 for several catalysts obtained from different precursors. In order to obtain a catalyst with high dispersion, preparation of the precursor should be carried out under relatively severe conditions.

Catalytic Activity and Selectivity

Catalytic activities (r_0) and selectivities (OY) of modified Ni–SiO_2 (1 : 1) catalysts in enantioselective hydrogenation of methyl acetoacetate were plotted in Fig. 11 as functions of the $NiCO_3$ content in the precursors. The activity decreased with an increase in $NiCO_3$ content in accord with the decrease in metal surface area of the catalyst. Therefore, precursors should be prepared under relatively severe conditions in order to obtain highly active catalysts. The enantioselectivity of the catalysts reduced at 400°C for 3 h increased with an increase in $NiCO_3$ content up to ca. 40% as expected and then decreased in spite of the increase in $\bar{D}_c$. When the catalysts were reduced under milder conditions, the optimum composition of the precursor was shifted to a higher proportion of $NiCO_3$ in accord with the change in $\bar{D}_c$ under different reduction conditions. The decrease in OY with increasing percentage of $NiCO_3$ beyond the optimum value can be explained by the decrease in the activity of larger crystallites with high selectivity as well as the increase in the contribution of smaller crystallites with low selectivity to overall hydrogena-

TABLE 2

BET and Metal Surface Areas of Ni–SiO_2 (1 : 1) Catalysts Obtained from Various Precursors

Catalyst No.	$NiCO_3$ content in precursor (%)	Surface areas[a]	
		BET	Metal
1	7	290	46
2	18	286	49
3	27	301	41
4	38	290	24
5	58	229	21
6	78	161	8

[a] Normalized to m²/g catalyst.

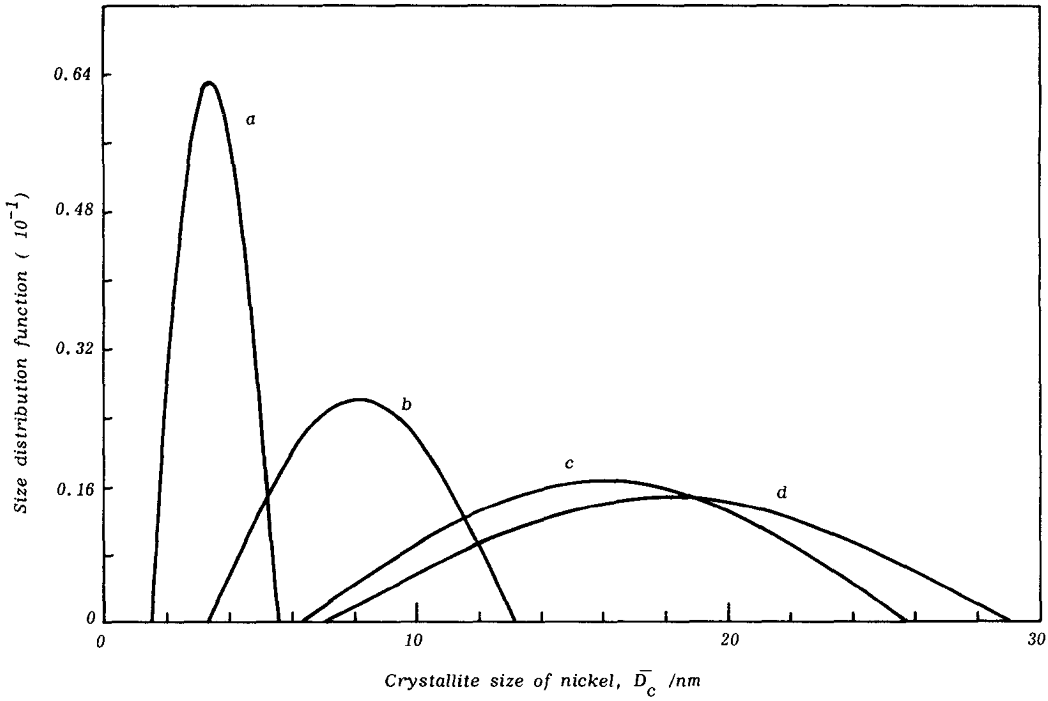

FIG. 10. Crystallite size distributions of nickel in Ni–SiO$_2$ catalysts obtained from various precursors with different NiCO$_3$ contents: (a) 18%, (b) 37%, (c) 58%, and (d) 78%.

tion. An increase in the proportion of NiCO$_3$ means a decrease in Ni(OH)$_2$ loading on SiO$_2$, which will bring about a progressive decrease in the size of relatively small crystallites originating from Ni(OH)$_2$. Accordingly, a high NiCO$_3$ content in the precursor will lead to a broad or a bimodal distribution of nickel crystallites in the reduced catalyst, though the CSDs in Fig. 10 do not show the existence of so small crystallites because of the limit of the method employed. In other words, the enantioselective hydrogenation can be used as a probe of CSD of nickel in a catalyst because this reaction is highly structure-sensitive as reported previously (*14–17*).

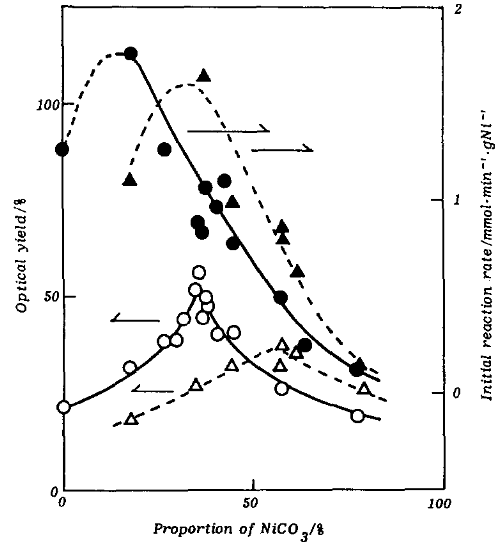

FIG. 11. Dependence of the activity (●, ▲), and the enantioselectivity (○, △) of modified Ni–SiO$_2$ catalysts on the composition of catalyst precursors. (●, ○) Reduced at 400°C for 3 h; (▲, △) reduced at 300°C for 1 h.

CONCLUSIONS

1. Thermal gravimetric analysis (TGA) was found to be quite useful to establish the chemical composition of catalyst precursors and also to determine the reducibility

of supported catalysts under various reduction conditions by using H_2 flow.

2. Almost all preparation variables affect the composition of precipitated precursors of Ni–SiO_2 catalysts. The proportion of $NiCO_3$ in a precursor, basic nickel carbonate, decreases as the preparation conditions become severe.

3. The reducibility of the $Ni(OH)_2$-rich precursor is lower than that of the $NiCO_3$-rich precursor probably because of the stronger metal–support interaction between $Ni(OH)_2$ and SiO_2. A precursor with the higher proportion of $NiCO_3$ results in a catalyst with the larger mean crystallite size of nickel after H_2 reduction.

4. The hydrogenation activity strongly depends on the preparation conditions such as precipitation and drying temperatures. The precursors should be prepared under relatively severe conditions in order to obtain highly dispersed and active catalyst after H_2 reduction.

5. The selectivity of a Ni–SiO_2 (1 : 1) catalyst in the enantioselective hydrogenation of methyl acetoacetate vary with the $NiCO_3$ percentage in the precursor. This can be explained in terms of the crystallite size distribution of nickel in the catalysts.

ACKNOWLEDGMENTS

The authors wish to thank Mr. Kazuo Fukuda for help in the X-ray line profile analysis and Mr. Teruo Utsumi for his experimental assistance.

REFERENCES

1. Schuit, G. C. A., and van Reijen, L. L., "Advances in Catalysis," Vol. 10, p. 242. Academic Press, New York, 1958.
2. Morikawa, K., Shirasaki, T., and Okada, M., "Advances in Catalysis," Vol. 20, p. 97. Academic Press, New York, 1969.
3. Martin, G.-A., Imerik, B., and Prettre, M., *J. Chim. Phys. Phys.-Chim. Biol.* **66**, 1682 (1969).
4. Coenen, J. W. E., and Linsen, B. G., *in* "Physical and Chemical Aspects of Adsorbents and Catalysts" (B. G. Linsen, Ed.), p. 471. Academic Press, New York/London, 1970.
5. Richardson, J. T., and Dubus, R. J., *J. Catal.* **54,** 207 (1978).
6. Nozawa, I., and Shirasaki, T., *Nippon Kagaku Kaishi,* 1062, 1066 (1978).
7. Nozawa, I., *Nippon Kagaku Kaishi,* 568 (1979).
8. Hermans, L. A. M., and Geus, J. W., *in* "Preparation of Catalysts II" (B. Delmon, P. Grange, P. Jacobs, and G. Poncelet, Eds.), p. 113. Elsevier, The Netherlands, 1979.
9. Houalla, M., Delannay, F., Matsuura, I., and Delmon, B., *J. Chem. Soc. Faraday Trans. 1* **76,** 2128 (1980).
10. Martin, G. A., Mirodatos, C., and Praliaud, H., *Appl. Catal.* **1,** 367 (1981).
11. Houalla, M., *in* "Preparation of Catalysts III" (G. Poncelet, P. Grange, and P. A. Jacobs, Eds.), p. 273. Elsevier, The Netherlands, 1983.
12. Montes, M., P. de Bosscheyde, Ch., Hodnett, B. K., Delannay, F., Grange, P., and Delmon, B., *Appl. Catal.* **12,** 309 (1984).
13. Blackmond, D. G., and Ko, E. I., *Appl. Catal.* **13,** 49 (1984).
14. Mallya, R. M., and Murthy, A. R. V., *J. Indian Inst. Sci.* **43,** 65 (1961).
15. Nitta, Y., Sekine, F., Imanaka, T., and Teranishi, S., *Bull. Chem. Soc. Jpn.* **54,** 980 (1981).
16. Nitta, Y., Sekine, F., Imanaka, T., and Teranishi, S., *J. Catal.* **74,** 382 (1982).
17. Nitta, Y., Yamanishi, O., Sekine, F., Imanaka, T., and Teranishi, S., *J. Catal.* **79,** 475 (1983).
18. Nitta, Y., Utsumi, T., Imanaka, T., and Teranishi, S., *Chem. Lett.,* 1339 (1984).
19. Izumi, Y., Harada, T., Tanabe, T., and Okuda, K., *Bull. Chem. Soc. Jpn.* **44,** 1418 (1971).
20. Moraweck, B., De Montgolfier, Ph., and Renouprez, A. J., *J. Appl. Crystallogr.* **10,** 184, 191 (1977).
21. Shimomura, Y., Tsubokawa, I., and Kojima, M., *J. Phys. Soc. Jpn.* **9,** 521 (1954).
22. Wendt, G., Siegel, H., and Schmitz, W., *Cryst. Res. Technol.* **17,** 1435 (1982).
23. Senderens, J. B., and Aboulenc, J., *Bull. Soc. Chim. Fr.* **11,** 641 (1912).
24. Lorenz, P., Finster, J., Wendt, G., Salyn, J. V., Zumadilov, E. K., and Nefedov, V. I., *J. Electron Spectrosc. Relat. Phenom.* **16,** 267 (1979).
25. Montes, M., Soupart, J.-B., De Saedeleer, M., Hodnett, B. K., and Delmon, B., *J. Chem. Soc. Faraday Trans. 1* **80,** 3209 (1984).